

Remarkable Enhancement in Electrochemical Performances of La-Mg-Ni-based Alloy Decorated with the Reduced Graphene Oxide Supported Cobalt

Dongyuan Huang¹, Bing Wei¹, Peilin Qing^{2,*}, Wenzheng Zhou^{1,2}, Haizhen Liu^{1,2}, Jin Guo^{1,2}, Zhiqiang Lan^{1,2,*}

¹ Guangxi Novel Battery Materials Research Center of Engineering Technology, Guangxi Key Laboratory of Processing for Non-ferrous Metallic and Featured Materials, Guangxi Colleges and Universities Key Laboratory of Novel Energy Materials and Related Technology, School of Physical Science and Technology, Guangxi University, Nanning 530004, P. R. China

² Guangxi Colleges and Universities Key Laboratory of structure research and performance development of rare earth alloy, School of Materials Science and Engineering, Baise University, Baise 533000, P. R. China

*E-mail: plqing110@163.com (Peilin Qing) and l_zq1100@163.com (Zhiqiang Lan)

Received: 8 April 2020 / Accepted: 22 May 2020 / Published: 10 July 2020

A reduced graphene oxide supported cobalt (Co@G) was synthesized via a wet-chemical method and was then introduced into a La_{0.7}Mg_{0.3}(Ni_{0.85}Co_{0.15})_{3.5} alloy (designated as La-Mg-Ni) by means of mechanical alloying. Experimental results indicated that the La-Mg-Ni alloy electrodes decorated with Co@G nanocomposites exhibited excellent electrochemical performance. At a discharge current density of 1200 mA/g, the high rate dischargeability (*HRD*₁₂₀₀) of the undecorated alloy electrode was 59.8%. This value increased to 82.3%, 84.7%, and 70.7%, respectively, when the alloy electrode was decorated with *x* wt.% (*x*=3,6,9) Co@G nanocomposites, respectively. The exchange current density (*I*₀) and the limiting current density (*I*_L) were also enhanced under the catalytic action of the Co@G nanocomposites. The electrode decorated with the 6.0 wt.% Co@G nanocomposite exhibited the best electrochemical performance. The improvements in electrochemical performance of the La-Mg-Ni alloy electrodes are attributed to the synergistic catalytic action of graphene and Co, thereby facilitating the electron transport and shortening the ion transportation paths in the alloy electrodes.

Keywords: Battery; Electrochemical performance; Dynamics; Graphene; Rare earths

1. INTRODUCTION

Hydrogen energy is environmentally friendly, green, and cheaper than conventional energy sources and, accordingly, has attracted considerable attention. As a typical representative of hydrogen

energy applications, La-Mg-Ni-based hydrogen storage alloys have attracted significant interest [1–13]. Li et al. [1] suggested that the electrochemical performance of Ni-MH batteries can be improved via chemical element substitution. They found a new A_7B_{23} type layered structure, containing $[AB_5]$ and $[A_2B_4]$ units in a $La_2Mg(Ni_{0.8},Co_{0.2})_9$ alloy, which is effective in inhibiting alloy pulverization caused by hydrogen absorption. The Mg-containing alloy was more resistant to pulverization than the Mg-free alloy. Moreover, the cycle stability of the La-Mg-Ni alloy can be prolonged by reducing the deviation value of A_2B_4 and AB_5 subunits and corrosion of the alloying element Mg [3]. Chan et al. [5] indicated that the charge-discharge cycle stability of a La-Mg-Ni alloy was greatly influenced by the amount of AB_5 addition. When doping with 50 wt.% of AB_5 , the La-Mg-Ni alloy exhibited the maximum hydrogen storage capacity and the optimal cycle stability. Element substitution has been employed to enhance the electrochemical properties of Ni-MH batteries. The results of the study revealed that Ce replacement of La can reduce the pulverization and improve the cycle life of the Ni-MH batteries [6]. Partial substitution of Al for Co in a La-Mg-Ni-Co alloy led to a decrease in the discharge capacity, but an improvement in the cycle life of the electrode [8]. As an important metal element, Co (in small amounts) can improve the electrochemical capacity and increase the discharge plateau voltage [10]. The discharge capacity and the cycle life (S_{100}) of a $La_{0.75}Mg_{0.25}Ni_{3.5}$ alloy increased from 343.62 mAh/g to 388.7 mAh/g and from 51.45% to 61.1%, respectively, when Ni was partially replaced by Co [13]. Although the electrochemical properties of La-Mg-Ni-based electrodes have been significantly improved, these properties are still inadequate for meeting the demands of practical applications. Therefore, further research on these electrodes is necessary.

Graphene is characterized by outstanding attributes such as remarkable electron mobility, high specific surface, and excellent heat transfer performance. Therefore, graphene has been applied as catalysts to enhance the electrochemical properties of lithium sulfur batteries [14–16], Li-ion batteries [17–20], and supercapacitors [21, 22]. Similarly, graphene has been applied to Ni-MH batteries [2, 23–27]. Ouyang et al. [25] reported that the discharge capacity and the high-rate dischargeability of La-Mg-Ni electrodes are enhanced through doping with graphene. Additionally, reduced graphene oxide supported Nickel (Ni@rGO) nanocomposites result in enhanced electrochemical properties of La-Mg-Ni electrodes [27]. We found that the reduced graphene oxide supported nickel was more effective than nickel or graphene alone in improving the electrochemical performance of the La-Mg-Ni system. In particular, Ni@rGO nanocomposites with a porous structure are conducive to hydrogen atom diffusion, thereby improving the electrochemical kinetic properties of the electrodes. As previously mentioned, graphene plays a crucial role in improving the electrochemical performance of electrodes. Cobalt (Co) has been used as an additive to improve the electrochemical performance of La-Mg-Ni electrodes. Therefore, we conclude that graphene supported cobalt catalysts may be adopted as an excellent additive for enhancing the electrochemical properties of La-Mg-Ni alloy electrodes. In this work, a reduced graphene oxide supported cobalt (Co@G) nanocomposite was prepared by means of a wet-chemical method. This nanocomposite was introduced into a La-Mg-Ni electrode to investigate the effects of the Co@G nanocomposite on the electrochemical performance of the La-Mg-Ni electrode.

2. EXPERIMENTAL

2.1. Preparation of Co@G nanocomposites

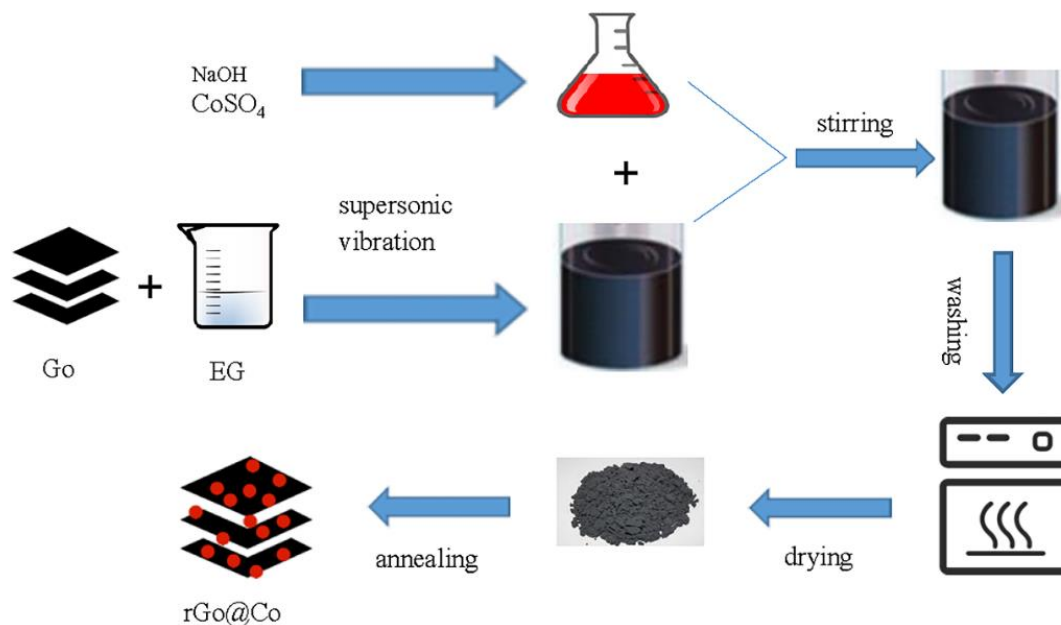


Figure 1. Preparation process of Co@G nanocomposite

Figure 1 shows the preparation process of the Co@G nanocomposites. In the first step, 0.5 g of graphene oxide was added to 25 mL of ethylene glycol solution. The solution was then subjected to 1 h of ultrasonic vibration in order to form a stable graphene oxide suspension. Afterward, 24 mL of Co sulfate hexahydrate solution (1 mol/L) and sodium hydroxide solution (5 mol/L) were injected into the obtained graphene oxide suspension and mixed for 30 min in a magnetic stirring reactor. The suspension of graphene oxide/Co was obtained by means of centrifugation and washed five times in deionized water. The washed samples were then heated for 12 h at 160 °C in a drying oven and then cooled to ambient temperature. Subsequently, the dried products were heated at 750 °C for 3 h in a mixture gas (Ar:H₂=93:7) and were designated as Co@G nanocomposites.

2.2. Preparation of the La_{0.7}Mg_{0.3} (Ni_{0.85}Co_{0.15})_{3.5} electrode

A La_{0.7}Mg_{0.3} (Ni_{0.85}Co_{0.15})_{3.5} alloy was prepared by means of magnetic induction melting under argon atmosphere protection. La, Ni, and Co blocks were used as raw materials, and Mg was replaced with a MgNi₂ alloy. The purity of all the raw materials or alloy was >99 wt.%. To compensate the loss of Mg element during the smelting process, the mass of Mg is increased by 10%. To ensure the uniform distribution of each component in the alloy, the alloy was melted three times. The melted alloy ingot was ground to a powder (particle size: 200 mesh) and divided into four parts. Four powders were obtained by adding a Co@G nanocomposite with x ($x=0, 3$ wt.%, 6 wt.%, and 9 wt.%) to each part.

Subsequently, the powders were placed in a jar and milled at a speed of 300 rpm for 10 min with a ball to powder ratio of 20:1. The resulting powder was mixed with a carbonyl nickel powder in a weight ratio of 1:4, and the mixture was then pressed into rounded electrodes under a pressure of 20 MPa.

2.3. Characterization

The phase composition of the samples was determined via X-ray diffraction (XRD; Miniflex 600, Rinku; CuK α radiation at 40 kV and 200 mA). Furthermore, the morphology of the catalyst was examined by means of scanning electron microscopy (SEM; JSM-6510A). The corresponding electrochemical properties were measured using a three-electrode open cell containing a counter electrode (NiOOH/Ni(OH)₂), reference electrode (Hg/HgO), and working electrode (metal hydride electrode). For the measurements, the working electrodes were immersed for 24 h in 6 mol/L of KOH aqueous solution to allow full wetting of each electrode. The electrodes were then charged at a current density of 100 mA/g for 4 h. Subsequently, each electrode was discharged for 10 min at a current density of 80 mA/g to a cut-off voltage of -0.5 V (vs. reference electrode) for activation. The cycle stability and high rate dischargeability of the electrodes were measured on an HTEST electrochemical workstation at ambient temperature. Polarization curve measurements of the electrode were performed by scanning the electrode potential from -5 mV to 5 mV at a rate of 0.1 mV/s and 50% depth of discharge (DOD). Potentiodynamic potential polarization curves were plotted by scanning the work electrodes (scanning rate: 10 mV/s) from -0.3 V to 1.0 V. The cyclic voltammetry measurements were performed by scanning the alloy electrodes (scanning rate: 5 mV/min) from -1.2 to 0.0 V (vs. Hg/HgO) on a Reference-1000 electrochemical workstation.

3. RESULTS AND DISCUSSION

Fig. 2 shows the XRD patterns of the La_{0.7}Mg_{0.3}(Ni_{0.85}Co_{0.15})_{3.5} alloy and Co@G nanocomposites. The alloy consisted mainly of La₂Ni₇ and LaNi₅ phases. For the as-prepared Co@G nanocomposites, the diffraction peaks corresponding to Co element occurred at $2\theta=44.2^\circ$, 51.5° , and 75.8° . The characteristic peak, at $2\theta\sim 25.9^\circ$, of reduced graphene oxide occurred with very weak intensity in the Co@G (as shown in the inset of Fig. 2). The microstructure and elemental distribution of the as-prepared nanocomposites were investigated via SEM and EDS. As shown in the SEM images (Fig. 3a, b), numerous fine nanosized particles were anchored on the surface and embedded in the matrix of the sheet-structure material. The EDS analysis results revealed that these particles (Fig. 3c) and the sheet matrix (Fig. 3d) are graphene and Co particles, respectively. These results demonstrate that reduced graphene oxide supported Co nanocomposites have been successfully prepared by means of a wet-chemical method.

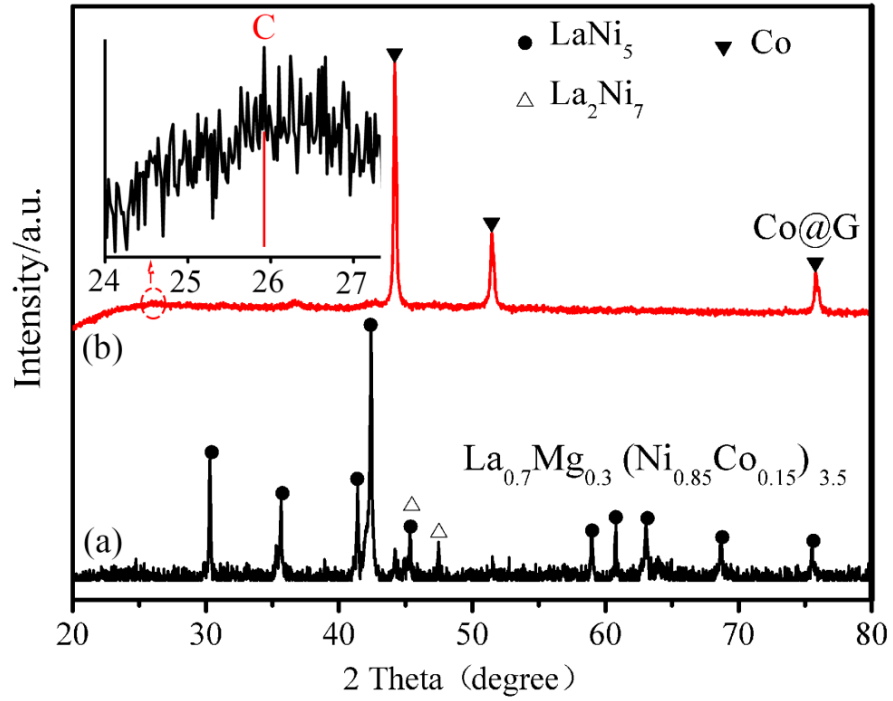


Figure 2. XRD patterns of $\text{La}_{0.7}\text{Mg}_{0.3}(\text{Ni}_{0.85}\text{Co}_{0.15})_{3.5}$ alloy and Co@G nanocomposites

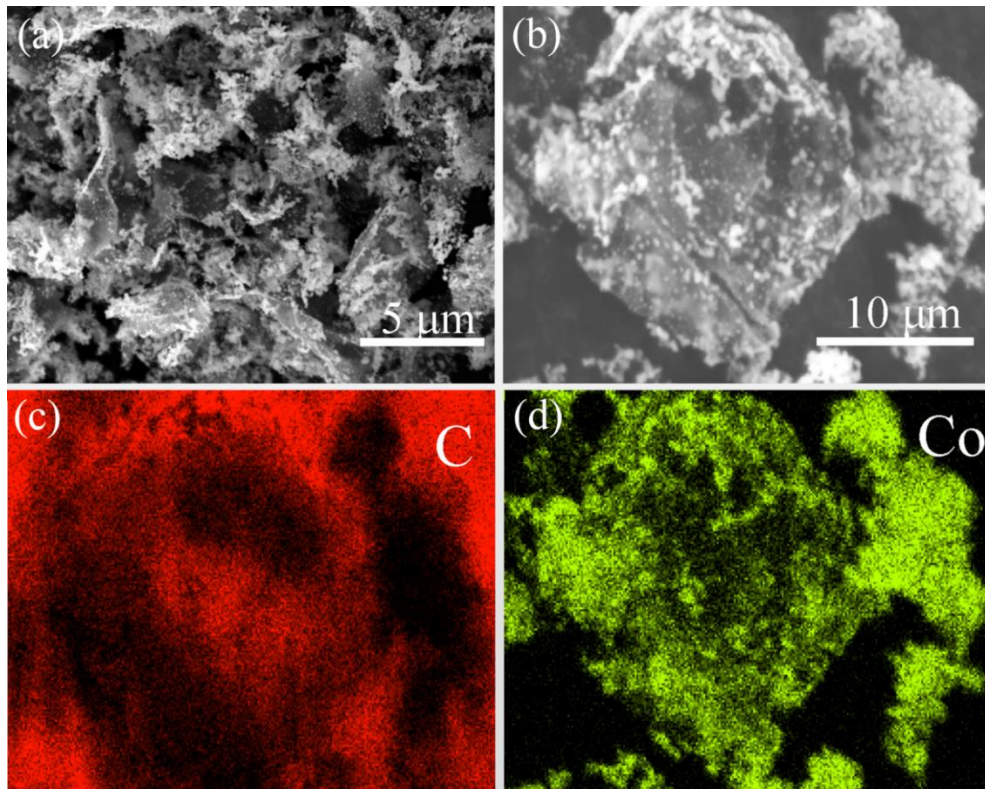


Figure 3. SEM images of Co@G nanocomposites (a, b) and EDS images of (c) C and Co elements

Figure 4 shows the discharge potential curves of the undecorated and Co@G nanocomposite decorated electrodes. With the addition of the Co@G nanocomposite, the discharge voltage platform was widened, indicating that the Co@G nanocomposite can enhance the discharge performance of the alloy electrode.

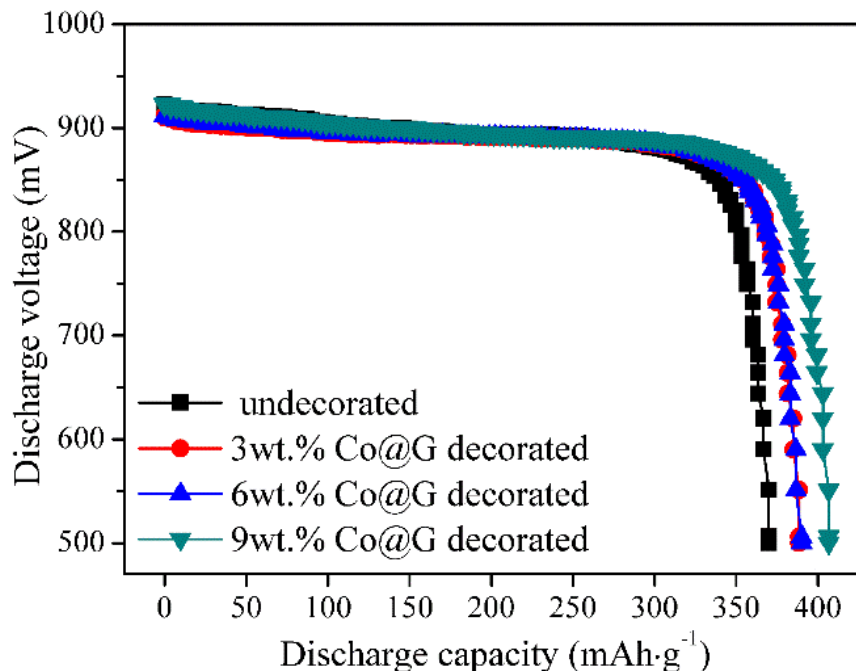


Figure 4. Discharge potential curves of the $\text{La}_{0.7}\text{Mg}_{0.3}(\text{Ni}_{0.85}\text{Co}_{0.15})_{3.5}$ alloy and Co@G-decorated electrodes

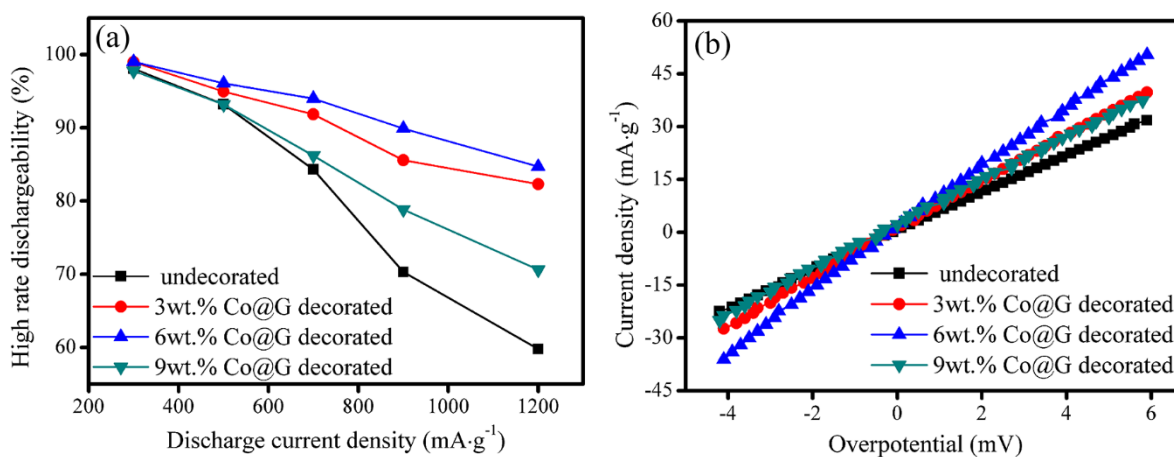


Figure 5. High rate dischargeability (a) and linear polarization curves (b) of the $\text{La}_{0.7}\text{Mg}_{0.3}(\text{Ni}_{0.85}\text{Co}_{0.15})_{3.5}$ alloy and Co@G-decorated electrodes

The maximum discharge capacity of the undecorated electrode (370.5 mAh/g) is higher than the value reported in reference [2]. This maximum discharge capacity increased to 390.8 mAh/g, 390.8 mAh/g, and 406.7 mAh/g when 3 wt.%, 6 wt.%, and 9 wt.%, respectively, of the nanocomposite were added to the electrode. Hence, the discharge capacity of the alloy electrode can be improved by adding

appropriate amounts of Co@G nanocomposites to the electrode. Zhang et al. [13] suggested that the addition of Co element to La-Mg-Ni alloy can increase the abundance of the LaNi₅ phase, leading to an increase in the discharge capacity of the La-Mg-Ni alloy electrodes. Additionally, the addition of graphene or reduced graphene oxide can enhance the discharge capacity of a Ni-MH battery [25, 27]. Therefore, the increase in the discharge capacity of the alloy can be attributed to the combined effect of the abundance characterizing the LaNi₅ phase and the presence of the graphene.

Fig. 5(a) shows the relationship between the high rate dischargeability (*HRD*) and discharge current density of the La_{0.7}Mg_{0.3}(Ni_{0.85}Co_{0.15})_{3.5} alloy and Co@G-decorated electrodes at different discharge current densities. As shown in the figure, the *HRD* value of each electrode decreased with increasing discharge current density. A *HRD* value of 84.3%, which is 7.5%, 9.7%, and 1.9% lower than that of the *x* wt.% (*x*=3,6,9) Co@G-decorated electrodes, respectively, was obtained for the undecorated alloy electrode (discharge current density: 700 mA/g). When the discharge current density increased from 700 mA/g to 1200 mA/g, the *HRD* value of the undecorated electrode decreased to 59.8%, corresponding to a reduction of 29.1%. The *HRD*₁₂₀₀ values of the *x* wt.% (*x*=3,6,9) Co@G-decorated electrodes (82.3%, 84.7%, and 70.7%) were 10.3%, 9.7%, and 17.8% lower, respectively, than that of the undecorated alloy. The *HRD*₁₂₀₀ value of the Co@G-decorated electrodes is larger than those of PANI-coated La-Mg-Ni-based alloy electrodes [28] and a La_{0.78}Mg_{0.22}Ni_{3.73} electrode reported by Han et al. [29]. The *HRD*₁₂₀₀ value of the as-cast La_{0.78}Mg_{0.22}Ni_{3.90} alloy electrode was ~78%, which is also lower than the values obtained for the *x* wt.% (*x*=3,6) Co@G-decorated electrodes [30]. These results demonstrated that the electrochemical kinetic properties of the La_{0.7}Mg_{0.3}(Ni_{0.85}Co_{0.15})_{3.5} electrode can be significantly improved by adding a Co@G nanocomposite to the electrode. Fig. 5(b) shows the linear polarization curves of the La_{0.7}Mg_{0.3}(Ni_{0.85}Co_{0.15})_{3.5} alloy and Co@G-decorated electrodes. The overpotential, which ranged from -5 mV to +5 mV, was linearly related to the polarization current density. The exchange current density (*I*₀) associated with the curves was determined as follows:

$$I_0 = I \frac{RT}{F\eta}$$

Where, *I*₀, *F*, *η*, *R*, and *T* are the exchange current density, Faraday constant, over potential, current density, gas constant, and absolute temperature, respectively. The values of *I*₀ were calculated and are listed in Table 1. *I*₀ values of 152.3 mA/g, 178.6 mA/g, 213.5 mA/g, and 173.6 mA/g were obtained for the bare electrode and the alloy decorated with 3 wt.%, 6 wt.%, and 9 wt.% of Co@G nanocomposites, respectively. In general, the electroactivity at the surface of the electrodes can be improved via surface treatment [31, 32]. For example, the *I*₀ of a La-Mg-Ni-based La_{0.88}Mg_{0.12}Ni_{2.95}Mn_{0.10}Co_{0.55}Al_{0.1} alloy electrode increased from 197.1 mA/g to 241.5 mA/g when the electrode was decorated with a Mo-Ni alloy [31]. Huang et al. [32] suggested that the electrocatalytic activity of Mg-Ni-La alloys can be enhanced by modifying the alloys with a graphene/silver (G/A) nanohybrid. The resulting *I*₀ of the G/A decorated Mg-Ni-La alloy electrode was 1.37 times larger than that of the bare alloy electrode. The addition of the Co@G nanocomposites promoted the diffusion of hydrogen atoms on the alloy electrode surface, resulting in improved electrochemical kinetics of the electrode. This was especially true for the electrodes decorated with 6 wt.% of Co@G nanocomposite, where the electrochemical dynamic properties were superior to those of the other electrodes. These findings are consistent with the results of *HRD*, indicating the significant role of reduced graphene oxide

supported cobalt doping in improving the electrochemical kinetics performance of the $\text{La}_{0.7}\text{Mg}_{0.3}(\text{Ni}_{0.85}\text{Co}_{0.15})_{3.5}$ electrode.

Table 1. Electrochemical kinetics parameters of $\text{La}_{0.7}\text{Mg}_{0.3}(\text{Ni}_{0.85}\text{Co}_{0.15})_{3.5}$ alloy and Co@G-decorated electrodes

Sample	I_p (mA/g)	I_L (mA/g)	I_0 (mA/g)	$HRD_{1200}/(\%)$
$\text{La}_{0.7}\text{Mg}_{0.3}(\text{Ni}_{0.85}\text{Co}_{0.15})_{3.5}$	1531.2	1139.8	152.3	59.8
3wt.% Co@G-decorated	2538.4	1452.9	178.6	82.3
6wt.% Co@G-decorated	2597.9	1879.0	213.5	84.9
9wt.% Co@G-decorated	2025.0	1779.7	173.6	70.7

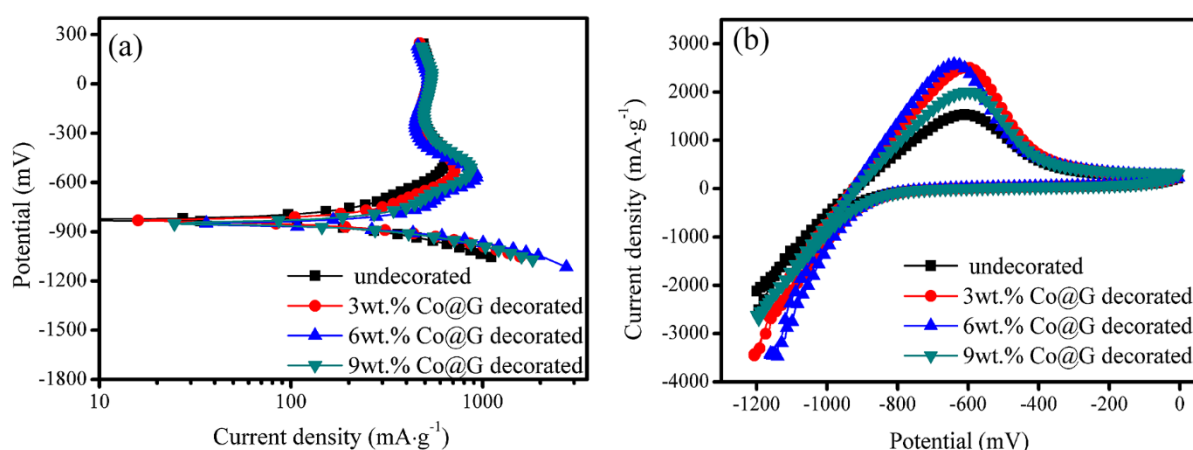


Figure 6. Potentiodynamic potential polarization curves (a) and the cyclic voltammogram curves (b) of the undecorated and Co@G-decorated nanocomposite electrodes

Fig. 6 shows the potentiodynamic potential polarization curves and the cyclic voltammogram curves of the $\text{La}_{0.7}\text{Mg}_{0.3}(\text{Ni}_{0.85}\text{Co}_{0.15})_{3.5}$ alloy and Co@G-decorated electrodes. The limiting current density (I_L) value of the undecorated electrode was 1139.8 mA/g (see Table 1). However, significant improvement was observed in the case of the Co@G-decorated electrodes. For example, I_L values of 1452.9 mA/g, 1879.0 mA/g, and 1779.7 mA/g, i.e., 1.27, 1.65, and 1.56 times the I_L of the undecorated electrode, were obtained for the x wt.%Co@G ($x=3,6,9$) nanocomposite decorated alloy electrodes, respectively. The diffusion ability of the hydrogen atoms in the alloy electrodes can be characterized by I_L , i.e., this ability increases with increasing I_L . Thus, the results indicate that the discharge and reaction kinetics performance of the bare alloy electrode can be significantly improved by decorating the electrode with Co@G nanocomposites. In particular, when decorated with 6 wt.% of the Co@G nanocomposites, the alloy electrode exhibited the optimal electrochemical dynamic performance. This is consistent with the HRD results shown in Fig. 5(a). Fig. 6(b) shows the cyclic voltammogram curves of the bare alloy and the Co@G-decorated electrodes. These curves revealed that the anodic oxidation peak current density (I_p) occurred at potential ranging from -650 mV to -550 mV. An anodic oxidation

peak current density of 1531.2 mA/g was calculated for the bare alloy electrode. For the electrodes with x wt.% Co@G ($x=3,6,9$) nanocomposites added this value increased to 2538.4 mA/g, 2597.9 mA/g, and 2025.0 mA/g, which were 1.66, 1.70, and 1.32 times larger, respectively, than that of the undecorated electrode. Generally, the anodic peak current density of the anode is used to characterize the electrocatalytic activity of the alloy electrode during the hydrogen oxidation process. The calculated I_p values revealed that the addition of the Co@G can enhance the electrocatalytic activity of the $\text{La}_{0.7}\text{Mg}_{0.3}(\text{Ni}_{0.85}\text{Co}_{0.15})_{3.5}$ alloy electrode, and this enhancement may be attributed to the following factors: (1) the dispersive Co nanoparticles on the reduced graphene oxide surface prevent stacking of the reduced graphene oxide, thereby facilitating electron transport in the alloy electrode; (2) the Co@G nanocomposites with a three-dimensional porous mesh structure can shorten ion transportation paths for the diffusion of electrolyte into electroactive materials.

4. CONCLUSIONS

A reduced graphene oxide supported cobalt nanocomposite was assembled via a wet-chemical method and used to decorate La-Mg-Ni alloy electrodes. The study results revealed that the electrochemical dynamic performance of the La-Mg-Ni alloy electrode can be enhanced significantly by decorating the electrode with Co@G nanocomposites. For example, when the electrode was decorated with 3 wt.%, 6 wt.%, and 9 wt.% Co@G nanocomposites, the HRD_{1200} value increased from 59.8% to 82.3%, 84.7%, and 70.7%, respectively. Similarly, the corresponding I_0 value increased from 152.3 mA/g to 178.6 mA/g, 213.5 mA/g, and 173.62 mA/g. Additionally, the electrocatalytic activity of the alloy electrode can be enhanced under the catalytic action of the Co@G nanocomposites. The anodic oxidation peak current density for x wt.% Co@G ($x=3,6,9$) decorated alloy electrodes was 1.66, 1.86, and 1.48 times as high as that of the undecorated sample. Suitable catalytic systems can yield improvement in the electrochemical dynamic performance of the La-Mg-Ni alloy electrode, and the La-Mg-Ni electrode decorated with 6.0 wt.% of Co@G nanocomposites exhibited the optimal integrated electrochemical performance.

References

1. Y Li, Z Liu, G Zhang, Y Zhang, H Ren, *J Power Sources*, 441(2019) 126667.
2. L Zeng, Z Lan, Z Sun, H Ning, H Liu, J Guo, *Int J Hydrogen Energy*, 44 (2019) 25840.
3. J Cao, Y M Zhao, L Zhang, Z R Jia, W F Wang, Z T Dong, S M Han, Y Li, *Int J Hydrogen Energy*, 2018, 43(37): 17800.
4. H Uesato, H Miyaoka, T Ichikawa, Y Kojima, *Int J Hydrogen Energy*, 44(2019) 4263.
5. K L Lim, Y Liu, Q A Zhang, K S Lin, S L I Chan, *J. Alloys Compd.*, 661(2016) 274.
6. W Lv, J Yuan, B Zhang, Y Wu, *J. Alloys Compd.*, 730(2018) 360.
7. L Kong, X Li, X Liao, X Cai, K Young, *J. Alloy. Compd.*, 792(2019) 260.
8. K Young, T Ouchi, L Wang, D F Wong, *J Power Sources*, 279(2015) 172.
9. Z Gao, Z Yang, Y Li, A Deng, Y Luo, H W Li, *Dalton Trans.*, 47(2018) 16453.
10. L Wang, K Young, T Meng, N English, S Yasuoka, *J. Alloys Compd.*, 664(2016)417.

11. J Liu, Y Yan, H Cheng, S Han, Y Lv, K Li, C Lu, *J Power Sources*, 351(2017) 26.
12. J Liu, S Han, Y Li, L Zhang, Y Zhao, S Yang, B Liu, *Int J Hydrogen Energy*, 41(2016) 20261.
13. Y H Zhang, D L Zhao, B W Li, X L Zhao, Z W Wu, X L Wang, *Int J Hydrogen Energy*, 33(2008)1868.
14. Y Wang, J Huang, J Lu, B Lu, Z Ye, *Electrochimica Acta*, 321(2019)134694.
15. F Qin, K Zhang, Z Zhang, J Fang, J Li, Y Lai, H Huang, *Ionics*, 25(2019)4615.
16. Z Wang, C Xu, L Chen, J Si, W Li, S Huang, Y Jiang, Z Chen, B Zhao, *Electrochim Acta*, 312(2019) 282.
17. K Han, Y Zhang, N Zhang, G Li, J Wang, G Xie, L Zhang, *J Nanosci Nanotechno.*, 20(2020) 2514.
18. S Yu, Z Wang, L Xiong, W Xiong, C Ouyang, *Phys Chem Chem Phys.*, 21(2019)23485.
19. Y Tang, J Chen, X Wang, X Wang, Y Zhao, Z Mao, D Wang, *Electrochim Acta*, 324(2019)134880.
20. F Khan, M Oh, J H Kim, *Chem Eng J.*, 369(2019)1024.
21. X Zheng, G Wang, F Huang, H Liu, C Gong, S Wen, Y Hui, G Zheng, D Chen, *Front chem.*,7(2019)1.
22. E Lai, X Yue, W Ning, J Huang, X Ling, H Lin, *Front chem.*, 7(2019) 660.
23. Y Nie, W Li, J Pan, R A Senthil, C Fernandez, A Khan, Y Sun, J Liu, *Electrochim Acta*, 289(2018) 333.
24. M M Li, Y Wang, C C Yang, Q Jiang, *Int J Hydrogen Energy*, 43(2018)18421.
25. L Z Ouyang, Z J Cao, L L Li, H Wang, J W Liu, D Min, Y W Chen, F M Xiao, R H Tang, M Zhu, *Int J Hydrogen Energy*, 39(2014)12765.
26. B Li, H Cao, J Shao, H Zheng, Y Lu, J Yin, M Qu, *Chem Commun.*, 47(2011)3159.
27. Z Lan, K Zeng, B Wei, G Li, H Ning, J Guo, *Int J Hydrogen Energy*, 42(2017)12458.
28. W Shen, S Han, Y Li, S Yang, Q Miao, *Appl Surf Sci.*, 258 (2012) 6316.
29. J Liu, Y Yan, H Cheng, S Han, Y Lv, K Li, C Lu, *J Power Sources*, 351(2017)26.
30. Y Zhao, S Han, Y Li, J Liu, L Zhang, S Yang, J Cao, Z Jia, *Electrochimica Acta*, 215(2016) 142.
31. Y Li, S Han, Z Liu, *Int J Hydrogen Energy*, 23(2010)12858
32. LJ Huang, YX Wang, Z Huang, JG Tang, Y Wang, JX Liu, JQ Jiao, JQ Liu, LA Belfiore, *J Power Sources*, 269(2014)716.
33. B V Ratnakumar, C Witham, R C Bowman Jr, A Hightower, B Fultz, *J Electrochem Soc.*,143(1996)2578.

© 2020 The Authors. Published by ESG (www.electrochemsci.org). This article is an open access article distributed under the terms and conditions of the Creative Commons Attribution license (<http://creativecommons.org/licenses/by/4.0/>).